



A novel precursory signal of the Central Pacific El Niño event: Eastern Pacific cooling mode

Lingjiang Tao^{1,2} · Wansuo Duan^{2,3}

Received: 18 October 2021 / Accepted: 24 February 2022

© The Author(s), under exclusive licence to Springer-Verlag GmbH Germany, part of Springer Nature 2022

Abstract

In recent decades, the tropical Pacific frequently experiences a new type of El Niño with warming center in the central tropical Pacific (i.e., the CP-El Niño) with distinct global climate effect to the traditional El Niño (i.e., EP-El Niño). Predicting the El Niño diversity is still a huge challenge for climatologists partly due to the precursory signals of El Niño events with different type is unclear. In the present study, a novel precursory signal of the CP-El Niño event that presents a negative sea surface temperature anomaly in the eastern tropical Pacific (i.e., EP-cooling mode) is revealed. The transition from the EP-cooling mode to CP-El Niño is explained by the basin-scale air–sea coupling in the tropical Pacific and teleconnections between the tropical and North Pacific. With the EP-cooling mode as a predictor, the forecast skill for the CP-El Niño in hindcast experiments is obviously improved by using regression models. The results in the present study are therefore instructive for promoting a better understanding of El Niño diversity and predictability.

1 Introduction

The El Niño–Southern Oscillation (ENSO) is recognized as one of the most prominent interannual variabilities in the climate system (Philander 1983) and has been extensively explored due to its profound global impacts [see the review by Wang (2019)]. After the 1990s, a new flavor of El Niño with the warming center in the central tropical Pacific (hereafter referred to as CP-El Niño), which is different from the conventional El Niño with a warming center in the eastern tropical Pacific (hereafter referred to as EP-El Niño), hoves into view of researchers [see the review by Timmermann et al. (2018)]. Though the CP-El Niño possesses a much smaller amplitude of sea surface temperature (SST) anomalies than the EP-El Niño, their climate effects are comparable and completely different in some regions (Ashok et al. 2007). Therefore, increasing efforts are focused on better

understanding the dynamics of different El Niño events. The EP-El Niño event has been suggested as a production of the fluctuation of thermocline as a result of basin-scale air–sea coupling in the tropical Pacific (Bjerknes 1969; Zebiak and Cane 1987). In contrast, the CP-El Niño event is more likely to be interpreted as resulting from the zonal advection feedback (Kug et al. 2009; Yu and Kim 2010; Duan et al. 2014); in particular, it was observed to be associated with the local development of wind and thermocline anomalies, thus suggesting a local air–sea coupling phenomenon (Kao and Yu 2009).

Beyond looking at the dynamics of different types of El Niño formations, the identification of the precursory signals is also vital to understand and predict El Niño diversities. Some studies have suggested that the precursory signals of El Niño events with different types originate from the extratropical Pacific (Ham et al. 2013; Ding et al. 2017; You and Furtado 2017; Wang et al. 2018, 2019a, b). For instance, a dipole structure of sea level pressure (SLP) variability over the North Pacific, known as the North Pacific Oscillation (NPO; Rogers 1981), has the ability to lead a CP-El Niño event (Yu and Kim 2011) through the “seasonal footprinting mechanism” (SFM) (Vimont et al. 2001, 2003a, b). Particularly, the NPO can impart a horseshoe SST footprint called the Victoria Mode (VM; Bond et al. 2003; Ding et al. 2015b) onto the North Pacific Ocean and influence the SST anomaly (SSTA) in the central tropical Pacific. Thus, the CP-El Niño

✉ Wansuo Duan
duanws@lasg.iap.ac.cn

¹ Department of Atmospheric and Oceanic Sciences and Institute of Atmospheric Sciences, Fudan University, Shanghai 200438, China

² LASG, Institute of Atmospheric Physics, Chinese Academy of Sciences, Beijing 100029, China

³ University of Chinese Academy of Sciences, Beijing 100049, China

events occurred frequently in recent decades as the NPO turns into dominant North Pacific climate variability (Yeh et al. 2015). While for the traditional El Niño event, its precursory signal is associated with the south Pacific, e.g., the Pacific–South American (PSA) pattern (Mo 2000) over the south Pacific that is found to have the potential to cause the positive SSTA in the eastern tropical Pacific after 1-year (Ding et al. 2015a).

Since extratropical climate variability is largely modulated by tropical SST variability (Alexander et al. 2002; Yu and Kim 2011), it is therefore inferred that distinct precursors to two types of El Niño may exist in the tropical Pacific. Several studies have reported that a basin-scale deepened thermocline and positive SSTA in the eastern tropical Pacific are most favorable for the generation of EP-El Niño events after 12 months (Mu et al. 2014; Hu and Duan 2016). Capotondi and Sardeshmukh (2015) emphasized the states of the thermocline anomalies in summer are the key to the formation of El Niño types; specifically, a deeper thermocline in the central Pacific and a shallower thermocline in the eastern Pacific at a two-season lead-time tend to induce a CP-El Niño event, while the reverse thermoclines tend to lead to an EP-El Niño event. Nevertheless, Yu and Kim (2010) focused on the evolution of the CP-El Niño and argued that the generation of CP-El Niño does not depend on the thermocline while its decay does. Recently, model sensitivity experiments indicated that whether a CP- or EP-El Niño will occur is dependent on the jointly effect of the westly wind bust and the thermocline (Fedorov et al. 2015). Obviously, the CP-El Niño precursory signal in the thermocline is still under debate.

The dispute regarding to the precursor of the CP-El Niño comes partly from the artificial definition of CP-El Niño itself. Many approaches have been proposed to separate EP-El Niño and CP-El Niño events (Ashok et al. 2007; Kao and Yu 2009; Kug et al. 2009; Ren and Jin 2011; Sullivan et al. 2016), leading to varying outcomes for El Niño types. Thus, the different precursors of CP-El Niño in previous studies are due in part to the definition of El Niño diversities that the authors adopted to some content. To avoid this confusion, a consensus analysis is preferred to classify the El Niño type and then to explore the common precursory signal of CP-El Niño regardless the various definitions. In the present study, the CP-El Niño precursory signal in the tropical Pacific is re-examined and analyzed with observations and model simulations. Particularly, a novel CP-El Niño precursory signal, i.e., the SST cooling mode in the eastern tropical Pacific (hereafter referred to as the EP-cooling mode) is reported to serve an optimal condition for the onset of CP-El Niño. Then, hindcast experiments are conducted to confirm the validity of the EP-cooling mode as a precursory signal for improving SST predictions associated with CP-El Niño events.

The rest of the paper is organized as follows. Section 2 describes the data and methods that are used to explore the different precursory signals of the CP- and EP-El Niño. In Sect. 3, the EP-cooling mode as CP-El Niño precursor is investigated using the observation and model simulations, followed by discussion in Sect. 4 on the involved dynamics of the transition from the EP-cooling mode to the CP-El Niño. In Sect. 5, the effect of the previous SSTAs in the eastern tropical Pacific on the ENSO prediction is examined based on the regression models. The paper will end with a summary and discussion in Sect. 6.

2 Data and methods

2.1 Data sets

In the present study, the reanalysis monthly data are adopted to explore the precursory signal of El Niño events in realistic. The monthly SST data are from the Met Office Hadley Centre Sea Ice and Sea Surface Temperature (HadISST) dataset (Rayner et al. 2003); the subsurface ocean data are from the Simple Ocean Data Assimilation (SODA, version 2.2.4) (Carton and Giese 2008); and the surface atmospheric and heat flux data are derived from the Twentieth Century Reanalysis (20CR) (Compo et al. 2011). All these data are linearly pre-detrended and analyzed during the period from January 1900 to December 2010, which is when the time series of the relevant data overlap. Anomalies of each physical variable field are obtained on an interannual scale by subtracting the climatological monthly mean from the above data, where the climatology is the climatological annual cycle derived from the corresponding variable data. In addition, the model data that are outputted from the preindustrial simulations by the Climate Model Intercomparison Project version 5 (CMIP5) are also adopted to examine the precursory signal of CP-El Niño events (see Table 1).

2.2 The definition of El Niño events with different types

The El Niño events in the present study are identified as those with a 3-month mean of the Niño 3.4 index (i.e., the averaged SSTAs over the Niño 3.4 region) greater than or equal to 0.5 °C that persists for at least five consecutive months. As mentioned in the introduction, the definitions of El Niño diversity vary. Hence, five frequently-used methods are adopted to determine the types of El Niño (Ashok et al. 2007; Kug et al. 2009; Sullivan et al. 2016; Ren and Jin 2011; Kao and Yu 2009). In Kug et al. (2009), a CP-El Niño year is defined when the Niño4 index is greater than Niño3 index in the peak phase, where the Niño3 index is referred as EP-El Niño index (EPI) and the Niño4 index is regarded

Table 1 Brief descriptions of the CMIP5 models adopted in the present study

Model	Institute	Data length (years)
ACCESS1-0	Centre for Australian Weather and Climate Research	500
ACCESS1-3	Centre for Australian Weather and Climate Research	500
bcc-csm1-1	Beijing Climate Center, China Meteorological Administration	500
CanESM2	Canadian Centre for Climate Modelling and Analysis	500
CCSM4	National Center for Atmospheric Research, USA	500
CESM1-BGC	NSF-DOE-NCAR, USA	500
CMCC-CMS	Centro Euro-Mediterraneo per I Cambiamenti Climatici,	500
CNRM-CM5	Centre National de Recherches Meteorologiques/Centre Europeen de Recherche et Formation Avancees en Calcul Scientifique	500
CSIRO-MK3-6-0	Commonwealth Scientific and Industrial Research Organization/Queensland Climate Change Centre of Excellence, Australia	500
EC-EARTH	European Centre	216
GFDL-ESM2G	Geophysical Fluid Dynamics Laboratory	500
GFDL-ESM2M	Geophysical Fluid Dynamics Laboratory	500
GISS-E2-H	NASA Goddard Institute for Space Studies	500
GISS-E2-R	NASA Goddard Institute for Space Studies	500
HadGEM2-CC	Met Office Hadley Centre	240
HadGEM2-ES	Met Office Hadley Centre	500
inmcm4	Institute for Numerical Mathematics	500
IPSL-CM5A-LR	Institut Pierre-Simon Laplace	500
IPSL-CM5A-MR	Institut Pierre-Simon Laplace	300
MIROC5	Atmosphere and Ocean Research Institute (The University of Tokyo), National Institute for Environmental Studies, and Japan Agency for Marine-Earth Science and Technology	500
MIROC-ESM	Atmosphere and Ocean Research Institute (The University of Tokyo), National Institute for Environmental Studies, and Japan Agency for Marine-Earth Science and Technology	500
MPI-ESM-LR	Max Planck Institute for Meteorology (MPI-M)	500
MPI-ESM-MR	Max Planck Institute for Meteorology (MPI-M)	500
MPI-ESM-P	Max Planck Institute for Meteorology (MPI-M)	500
MRI-CGCM3	Meteorological Research Institute	500
NorESM1-M	Norwegian Climate Centre (NorClim)	500

as CP-El Niño index (CPI). In Ashok et al. (2007), the CPI is indicated by $CPI = T_1 - 0.5 \cdot (T_2 + T_3)$, where T_1 is area-averaged SSTA over the central tropical Pacific (165° E–140° W, 10° S–10° N). T_2 and T_3 are respectively those over the eastern (110° W–70° W, 15° S–5° N) and western tropical Pacific (125° E–145° E, 10° S–20° N). Ren and Jin (2011) proposed a nonlinear indices based on the Niño3 and Niño4 indices as follows:

$$\begin{cases} EPI = Nino3 - \alpha \cdot Nino4 \\ CPI = Nino4 - \alpha \cdot Nino3 \end{cases}, \quad \text{where}$$

$$\alpha = \begin{cases} \frac{2}{5}, & Nino3 \cdot Nino4 > 0 \\ 0, & \text{otherwise} \end{cases}.$$

Similarly, Sullivan et al. (2016) used normalized Niño3 and Niño4 (denoted as Niño3n and Niño4n) to formulate CPI and EPI, namely, $EPI = Nino3n - 0.5 \cdot Nino4n$, $CPI = Nino4n - 0.5 \cdot Nino3n$. From Kao and Yu (2009), the CPI (EPI) is the principal component of leading mode in the tropical Pacific that is

filtered the linear effect of the SSTAs in the eastern (central) tropical Pacific. The types of El Niño events are thus classified by comparing the size of the CPI and EPI based on the above methods. Then, we used their consensus results to determine the type of El Niño among different methods. Finally, a total of 17 CP-El Niño and 15 EP-El Niño events are obtained during the period from January 1900 to December 2010 (see Table 2).

2.3 Statistical methods

To highlight the important role of the precursory signal in promoting the onset of CP-El Niño, the climate variability unrelated to the precursor should be verified to have little impact on the development of the CP-El Niño. In the present study, a filter technique is adopted to obtain the climate variability that is unrelated to the CP-El Niño precursor. This

Table 2 EP- and CP-El Niño events from 1900–2010 and their precursors

Year	Type	EP-cooling precursor	Year	Type	EP-cooling precursor
1902	CP	Y	1965	CP	Y
1904	CP	Y	1968	CP	Y
1905	EP	Y*	1969	EP	N*
1911	EP	Y*	1972	EP	Y*
1913	EP	Y	1976	EP	Y*
1914	CP	Y	1977	CP	Y*
1918	EP	Y*	1982	EP	N
1923	CP	Y	1986	EP	N*
1925	CP	Y	1987	CP	Y
1930	EP	Y	1991	CP	Y
1939	EP	N	1994	CP	Y
1940	CP	N*	1997	EP	N*
1941	EP	Y	2002	CP	Y*
1951	EP	Y*	2004	CP	Y
1957	CP	Y*	2006	EP	Y
1963	CP	Y	2009	CP	N*

The types of El Niño are determined according to the consensus among El Niño types identified by Ashok et al. (2007), Ren and Jin (2011) and Kao and Yu (2009) according to their proposed El Niño type definitions. “Y” denotes yes if the tropical Pacific has experienced an EP-cooling-like mode preceding a CP type or a non-EP-cooling mode preceding an EP-El Niño event; otherwise, “N” is indicated. And “*” indicates that the La Niña event occurs before the El Niño event. It can be found that 15 out of 17 CP-El Niño events are denoted by “Y”, indicating that these CP-El Niño events have an EP-cooling precursory signal, which indicates that the majority of the CP-El Niño events evolved from the EP-cooling mode

filter technique is described in Eq. (1), and the linear effect of $x(t)$ on $y(t)$ can be removed as follows:

$$y_{-x}(t) = y(t) - (\alpha + \beta \cdot x(t)) \quad (1)$$

where $y_{-x}(t)$ is the residual variability of $y(t)$ after removing the linear effect of $x(t)$ and α and β are obtained from the regression analysis between $x(t)$ and $y(t)$. Evidently, the residual variability $y_{-x}(t)$ is unrelated to $x(t)$. That is, if $x(t)$ is a precursor, $y_{-x}(t)$ is the climate variability that is part of $y(t)$ but unrelated to $x(t)$.

The significance of the correlation is determined using a two-tailed Student’s test, which involves the effective degree of freedom N_e proposed by Bretherton et al. (1999).

$$N_e = N \frac{1 - r_x r_y}{1 + r_x r_y}, \quad (2)$$

where r_x and r_y are the autocorrelation of variables x and y with lag 1, respectively, and N is the length of the variables. The composite analysis that confirms the result indicated by the correlation analysis is also performed.

3 Precursory signal of the CP-El Niño events

3.1 Observation

To classify the EP- and CP-El Niño life cycles in the observation, we conduct a lagged correlation of the wintertime CPI and EPI with the SST and wind anomalies in the tropical Pacific (see Figs. 1 and 2), where the EPI and CPI are obtained based on the definitions mentioned in Sect. 2. It is easily seen that the initial warmings of both EP- and CP-El Niño events, in accordance with the previous studies (e.g., Wang et al. 2019c; Yang et al. 2021), start from the western Pacific (WP) warming in the early year. Since the small perturbations of SST in the warm pool are easy to influence the atmosphere and trigger west wind anomalies, this western Pacific warming can be propagated eastward and amplified by the ocean current and the fluctuations of the thermocline. That is, the western Pacific warming tends to develop into an El Niño event via the zonal advection feedback and thermocline feedback processes. However, one can find that both EP- and CP-El Niño events can start from the WP warming, the WP warming therefore cannot act as an effective precursor to identify the El Niño types.

In fact, much early and different precursory signals of EP- and CP-El Niño events can be identified from the Figs. 1 and 2. Specifically, the early precursor of EP-El Niño event is associated with the basin-scale cooling event that could trigger western Pacific warming and subsequent Bjerknes mode [also see Bjerknes (1969) and Yu and Fang (2018)]. As the warm water accumulates eastward, the eastern Pacific of EP-El Niño is so discharged that it leads to a strong charge. The positive SSTA starts to decay rapidly and evolves into a double-year central Pacific cooling event again (Hu et al. 2014). Differed to the EP-El Niño, the early precursory signal of CP-El Niño is significantly related to a localized cooling event by 2 years ahead, i.e., a negative SSTA mode in the eastern tropical Pacific (hereafter referred to as the EP-cooling mode). What is worth noting is that the finding is robust for the most methods classifying types of El Niño. Therefore, a hypothesis is that the EP-cooling mode may be a precursory signal (at the 2-year lead) of the CP-El Niño, which is different from the initial warm signal with a 1-year lead time in the western-central tropical Pacific for the EP- and CP-El Niño.

To confirm the validity of the precursory EP-cooling mode of the CP-El Niño in identifying types of El Niño events in advance, we examine whether the tropical Pacific experienced an EP-cooling mode before each of the El Niño events. Here, the EP-cooling mode is defined as a negative and cooler SSTA in the eastern Pacific (110°W – 80°W , 5°S – 5°N) than the central tropical

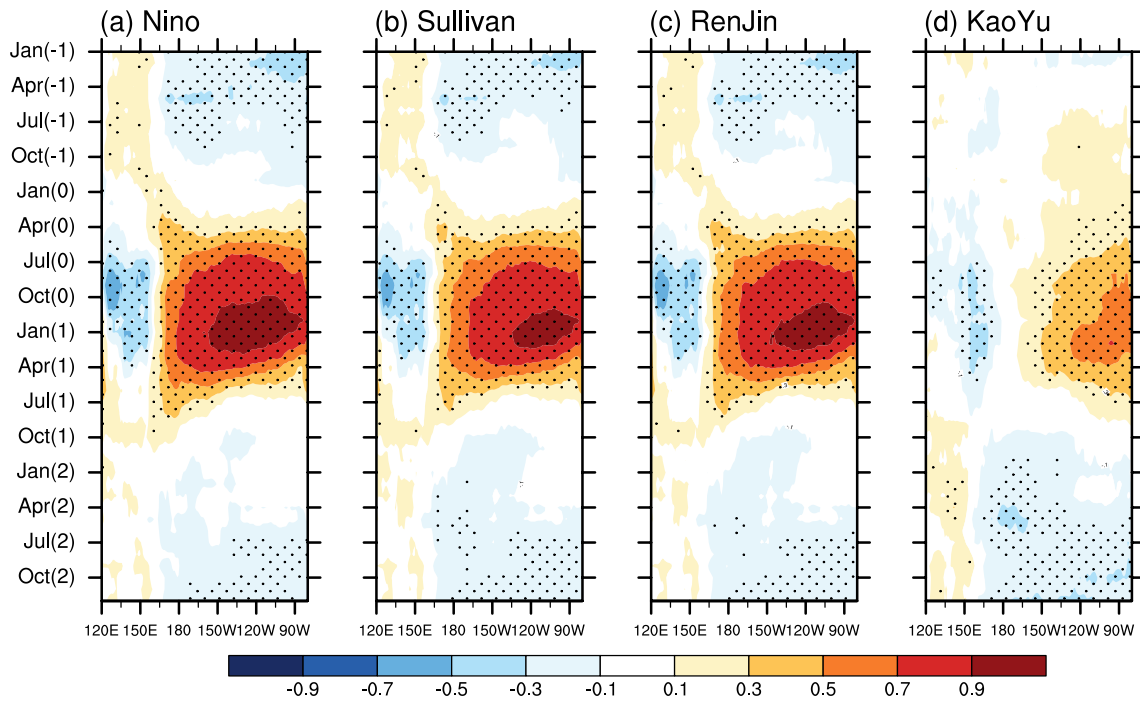


Fig. 1 Correlations between the equatorial SSTA and wintertime (December–January–February) EP-El Niño indices (EPIs) that are derived through the approaches proposed by **a** Kug et al. (2009), **b**

Sullivan et al. (2016), **c** Ren and Jin (2011) and **d** Kao and Yu (2009). The correlations above 95% confidence are dotted

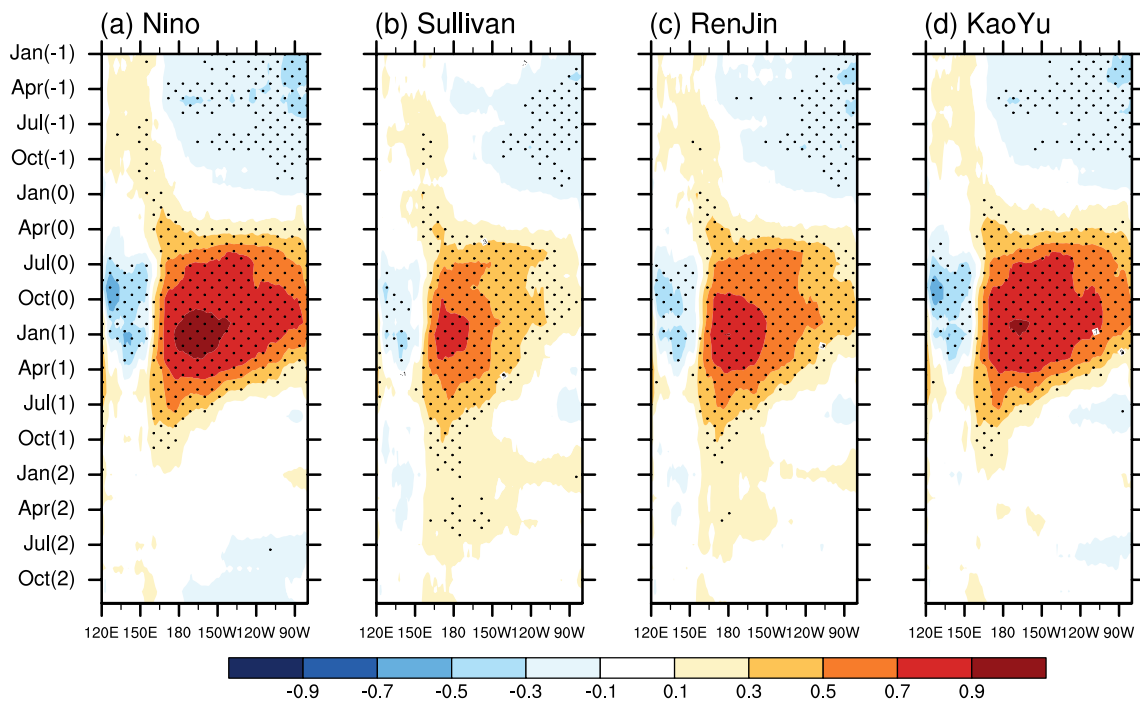


Fig. 2 Same as in Fig. 1 but for the CP-El Niño indices (CPIs)

Pacific (175° W–110° W, 5° S–5° N) from January–June. It is found that the majority of (88.2%) CP-El Niño events were evolved from the EP-cooling mode at 1–2 years lead time during 1900–2010 (see Table 2). Moreover, 67% of EP-El Niño events were unrelated to the previous EP-cooling mode. In addition, we also look at the La Niña events are preceding the El Niño events 2 years or not. In Table 2, the marker “*” indicates that the La Niña event occurs followed by the El Niño event. Consistent with the correlation analysis in Figs. 1 and 2, we can find that 60% EP-El Niño events occur after the La Niña events while the CP-El Niño events are unrelated to the previous La Niña events (only 5 out of 17 CP-El Niño events are originated from the La Niña events). The former results indicated that it is the EP-cooling mode not EP-La Niña that can be a reliable precursory signal for CP-El Niño. This information may provide important insights for classifying the type of upcoming El Niño event in advance.

3.2 Simulations from a corrected ENSO model

Evidently, it's not convincing to verify the distinct precursors of El Niño events by only analyzing the observation but without climate models. However, one undeniable fact is that current models still exhibit large biases in EP- and CP-El Niño simulations as well as their precursors (Taschetto et al. 2014; Wang et al. 2019c). Those model biases could confuse the detection of the precursors regarding to the CP- and EP-El Niño.

As other climate models, an intermediate coupled model (ICM) developed by Zhang et al. (2003) fails to simulate and predict the El Niño diversity (Tao et al. 2020). Since the model errors related to the CP-El Niño simulation are complicated, previous studies adopted the nonlinear forcing singular vector (NFSV)-assimilation approach to offset the combined effect of kinds of model errors of the ICM and constructed an ENSO model named as NFSV-ICM (Duan and Zhou 2013; Tao and Duan 2019). With the NFSV-ICM, the ENSO simulation and prediction towards El Niño diversities were significantly improved [see Duan et al. (2014), Tao and Duan (2019), and Tao et al. (2020)]. The NFSV-assimilation approach is used to deal with following minimum problems:

$$J(\mathbf{f}^*) = \min \sum_{t=0}^T \|\mathbf{M}_t(\mathbf{f}_t, \mathbf{u}_0) - \mathbf{u}_t^{obs}\|, \quad (3)$$

where \mathbf{u}_0 and \mathbf{u}_t^{obs} is the initial condition and observation, respectively; $\mathbf{M}_t(\mathbf{f}_t, \mathbf{u}_0)$ denotes the simulation result when a forcing \mathbf{f}_t is added to the total tendency of the forecast models. Clearly, \mathbf{f}^* represents the tendency perturbation that can offset the combined effect of kinds of model errors to the greatest extent when the J is close to 0. Then, with the

forcing \mathbf{f}^* , the corrected simulation can reproduce the climate events as observation.

In the present study, to reduce the model errors in El Niño simulations, \mathbf{f}^* is added to the tendency equation of SST to correct the model simulation. When the \mathbf{u}_t^{obs} is related to the CP-El Niño (EP-El Niño) events, the obtained \mathbf{f}^* could offset the combined effect of the model errors that are from the unsolved processes or uncertain mechanisms during the CP-El Niño (EP-El Niño) simulation using the ICM. We calculate the forcing \mathbf{f}^* for different CP-El Niño events of concerned time period and composite them for filtering the stochastic components, finally obtaining 12 monthly forcing vectors (denoted as CP-F). The CP-F thereby can capture the main effect of unsolved processes affecting CP-El Niño simulation in the ICM. The same approach is made for EP-El Niño and the relevant forcing vectors (denoted as EP-F) are obtained. Finally, EP-F and CP-F, like annual cycles of forcing, force the ICM, respectively, and finally formulate two NFSV-ICMs: one is the ICM with EP-F for EP-El Niño simulation while the other is the ICM with CP-F for CP-El Niño simulation. The free runs of EP- and CP-El Niño events made by the NFSV-ICMs are shown in Figs. 3 and 4. It is shown that the simulated EP- and CP-El Niño bear great resemblance to the observed ENSO cycle. The simulated EP-El Niño is associated with basin-scale cooling event (Fig. 3a). While for the CP-El Niño simulation, the precursor of CP-El Niño is related to the negative SSTAs in the eastern tropical Pacific (Fig. 3b). The results of NFSV-ICM simulations further verify the finding that the EP-cooling mode is the precursory signal of the CP-El Niño.

3.3 Simulations from CMIP6

As mentioned above, currently models have poor skills in ENSO diversity simulation, it will be difficult to link the EP-cooling precursor to the CP-El Niño events in the CMIP5 experiments. Still, we can focus on the changes in the El Niño warming center preceded by central Pacific cooling (CP-cooling) and EP-cooling modes to indicate whether a CP- or EP-El Niño will occur. A heat center index (HCI) is employed to quantify the position of the warming center of the SSTA as follows (Hu and Fedorov 2018):

$$\text{HCI} = \frac{\sum l \cdot T(l)}{\sum T(l)}, \quad (4)$$

where l is the longitude within 160–90° W and T is the averaged SSTA within 5° S to 5° N. Since the warming center of SSTA is only considered in the present study, $T(l)$ with negative values is set to zero to avoid the illusory impact of the negative SSTA on the determination of HCI.

Fig. 3 The long-time sections of equatorial SSTAs simulated by **a** the NFSV-ICM with EP-F and **b** CP-F. The contour intervals are 0.5 °C in **a** and 0.3 °C in **b**, respectively

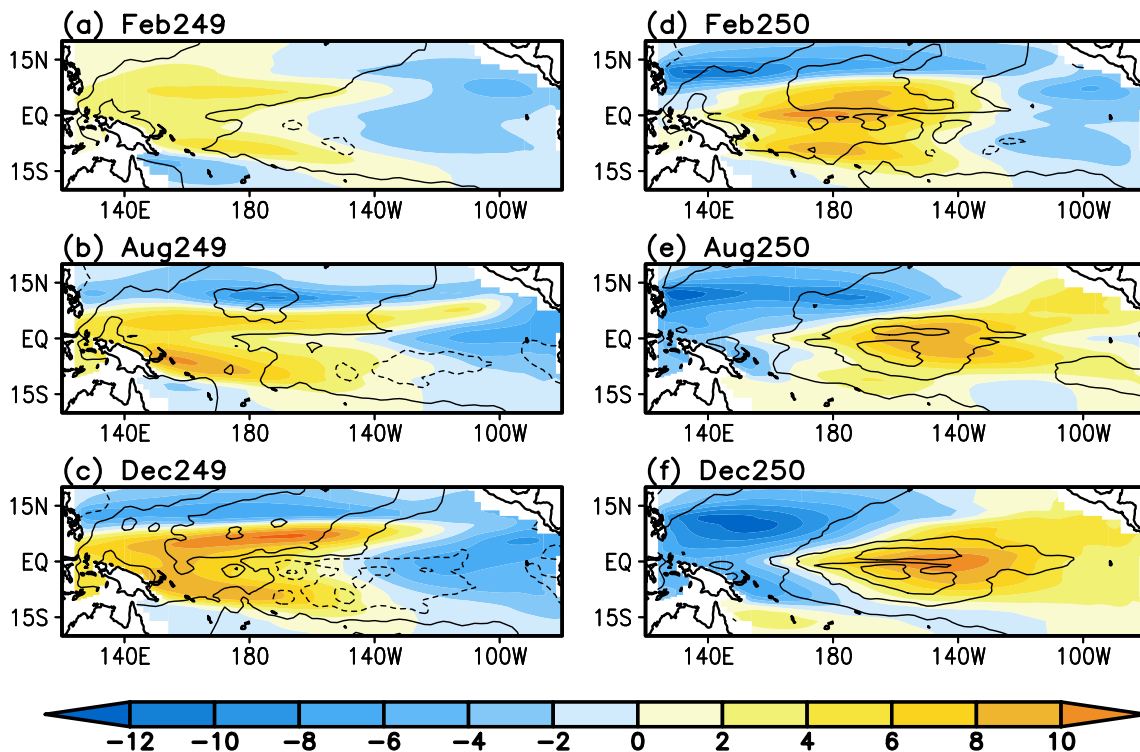
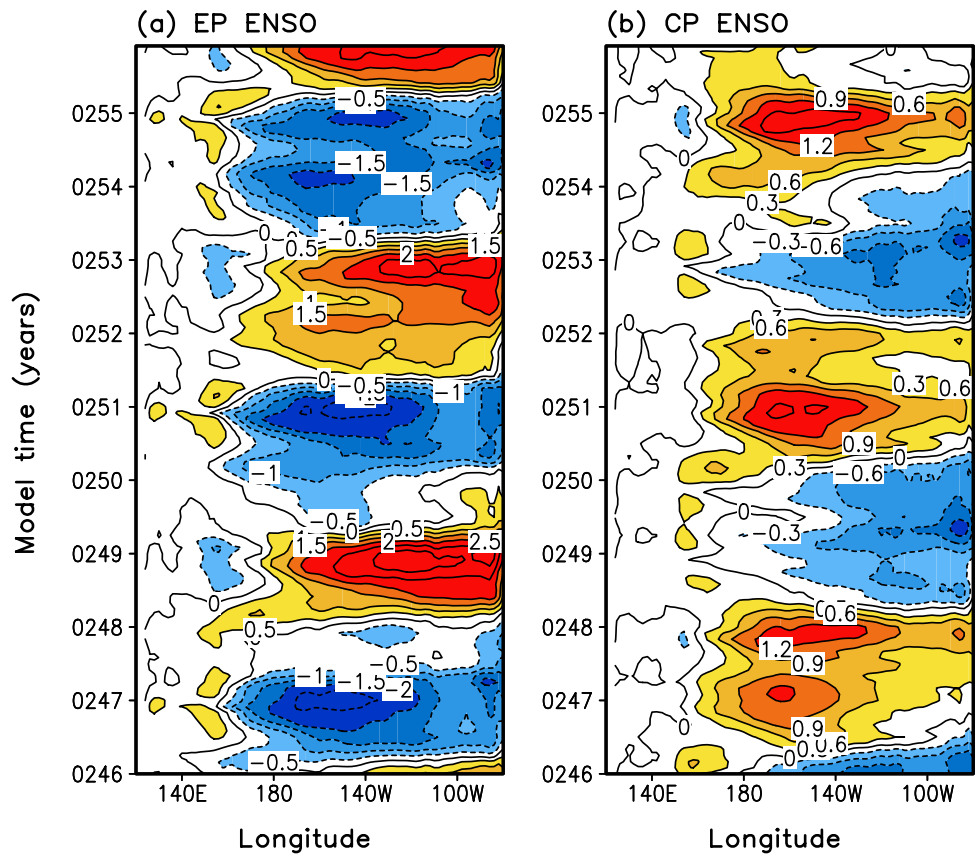


Fig. 4 Horizontal distributions of sea level anomaly (shaded) and subsurface temperature (contoured) of CP-El Niño simulation made by the NFSV-ICM with CP-F. The contour interval is 0.3 °C

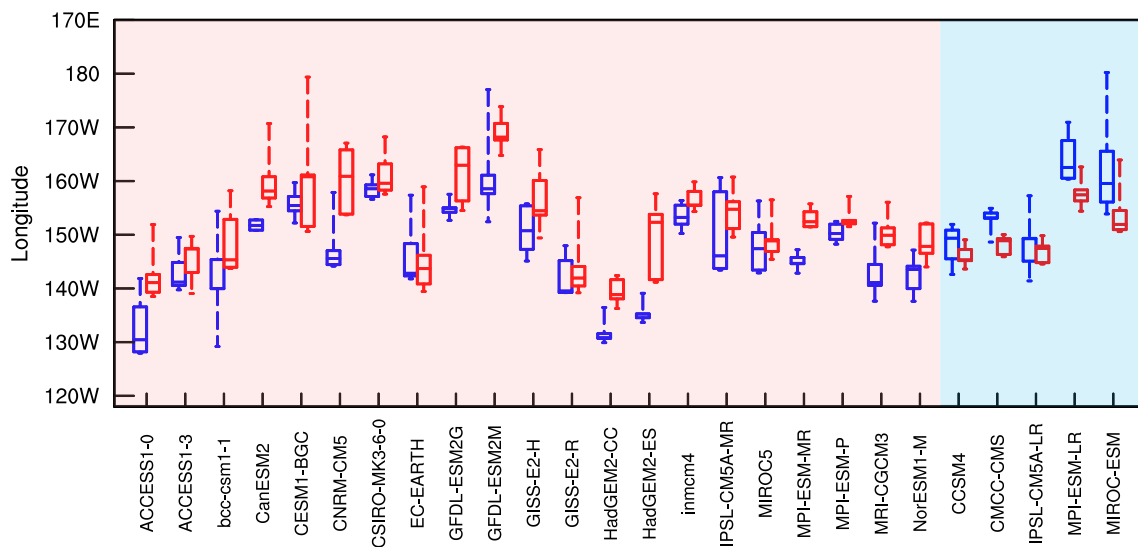


Fig. 5 Boxplot for the HCI of El Niño derived from the preindustrial simulations of CMIP5. Each model has two boxes: one is blue for the HCI after the CP-cooling-like mode; the other is red but for the HCI after the EP-cooling-like mode. An EP-cooling-like mode (a CP-cool-

ing-like mode) is defined as the negative SSTa in the eastern tropical Pacific (in the central tropical Pacific) less than the SSTa in the central tropical Pacific (in the eastern tropical Pacific)

The changes in the HCI of the El Niño events from each model are displayed in Fig. 5. It can be seen that 21 out of 26 models show that the location of the warming centers for the El Niño events originated from the EP-cooling mode are more west than those from the CP-cooling mode (Fig. 5). It is indicated that the previous negative SSTAs in the eastern tropical Pacific (i.e., the EP-cooling mode) favor future central Pacific SST warming.

Combining the observation and model simulations, we can confirm the hypothesis that the EP-cooling mode is a useful precursory signal of CP-El Niño-like events.

4 Mechanism to the precursory signal EP-cooling mode transitioning to CP-El Niño event

The previous section has fully corroborated the fact that the EP-cooling mode is the precursory signal of the CP-El Niño event, while the processes involved with such evolution is unclear. Therefore, in this section, we will examine how the cooling signal evolves into to a CP-El Niño event from the perspective of the air–sea interaction.

4.1 How does the EP-cooling mode evolve into CP-El Niño?

The transition from the SST cooling signal to the CP-El Niño-like event is possibly bridged by the subtropical Pacific warming that is induced by basin-scale easterly wind anomalies. Figure 6 displays the air–sea evolutions associated with

the CPI proposed by Ashok et al. (2007) as an example (Note: the CP-El Niño related air–sea evolution is similar when using different CPIs). The EP-cooling mode imposing on the climatological ocean enhances the zonal gradient of the equatorial SST, thereby accelerating the Walker circulation. Thus, southeasterly wind anomalies prevail over the equatorial Pacific (Fig. 6b), leading to anomalous mass transport towards the subtropical Pacific and western tropical Pacific. Infected by such V-shaped warming in the tropical subsurface, the tropical Pacific experiences a “Pacific meridional mode” (PMM; Chiang and Vimont 2004)-like air–sea coupling pattern that presents a dipole SSTa coupled with southwest wind anomalies in the eastern tropical Pacific (see Fig. 4c). The positive SSTa of the PMM can be maintained and amplified through a positive feedback known as the wind-evaporation-SST (WES) feedback (Xie and Philander 1994). Particularly, the anomalous westerly over the subtropical Pacific that acts to slack the trade wind tends to suppress evaporation and warm up the ocean, giving rise to the development of SSTa which will in turn feedback to the atmospheric and enhance the wind anomaly. The positive SSTa and anomalous westerly gradually invade into the central equatorial Pacific, leading to a strong zonal advection feedback, of which conditions are favorable for the formation of CP-El Niño events. Finally, the EP-cooling mode disappears and is replaced by a CP-El Niño-like event.

The former mechanism is also clearly revealed in the NFSV-ICM simulation. Take the CP-El Niño occurred in 250 as an example (Fig. 4). In the early stage (e.g., Feb249), the tropical Pacific is characterized by a shallowed thermocline and negative SSTa in the eastern

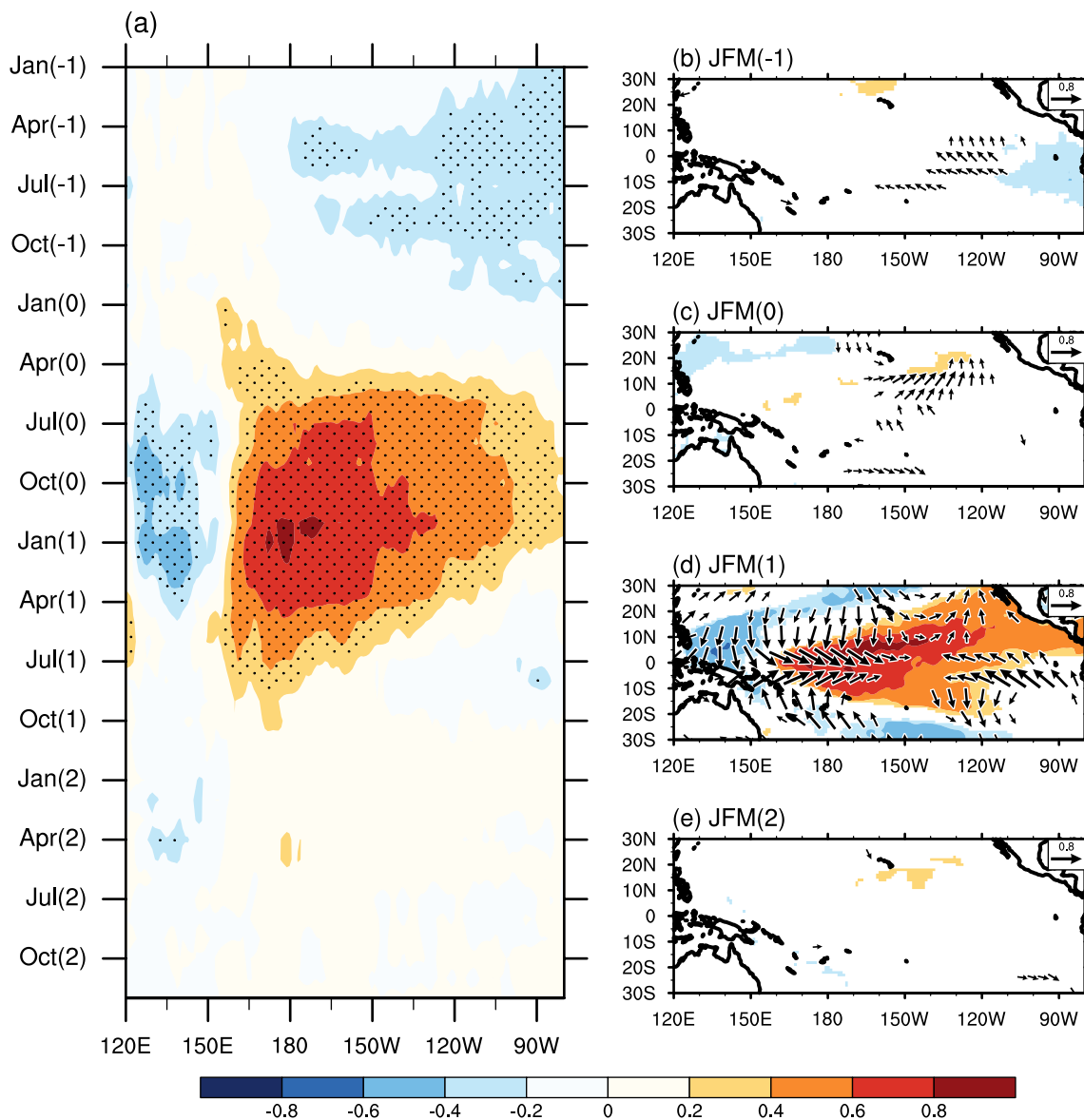


Fig. 6 Correlations between the wintertime (i.e., December–January–February) CPI and the tropical SST and surface wind anomalies. **a** Correlation of the wintertime CPI with tropical SST; and **b–e** horizontal distributions of the correlations of the wintertime CPI with the 3-month (i.e., January–February–March) averaged wind (vector) and SST (shaded). The CPI is the Modoki index proposed by Ashok et al. (2007). The bracketed number “0” denotes the correlation of the

wintertime CPI with the SST and wind anomalies in the same year; and “-1”, “1”, and “2” indicate the correlation of the wintertime CPI with the SST and wind anomalies in the last year, next year, and the year after next, respectively. The correlations above 99% confidence are dotted in **a**, and only correlations above 99% confidence are shown in **b–e**

tropical Pacific, i.e. the EP-cooling mode. In the meantime, the sea water, responding to the enhanced trade wind, is accumulated in the western tropical Pacific and off the equator. As a result, a significant subsurface warming exists in the subtropical Pacific (Fig. 4b, c), which can warm up the surface ocean gradually and formulate a PMM-like air–sea state as in the observation. The warming signal in the western Pacific is then displaced to the central Pacific by the zonal advection feedback (Fig. 4d,

e). Finally, a CP-El Niño event, originated from the EP-cooling mode, occurs in the Dec250.

The EP-cooling mode can also influence the atmospheric state over the North Pacific, thus favoring the development of SSTAs in the central tropical Pacific through the oceanic path. To examine the relationship between the precursory state in the tropical Pacific ocean and the North Pacific atmosphere, a cross-correlation is performed between the SSTAs (meridionally averaged over 5° S–5° N) along the

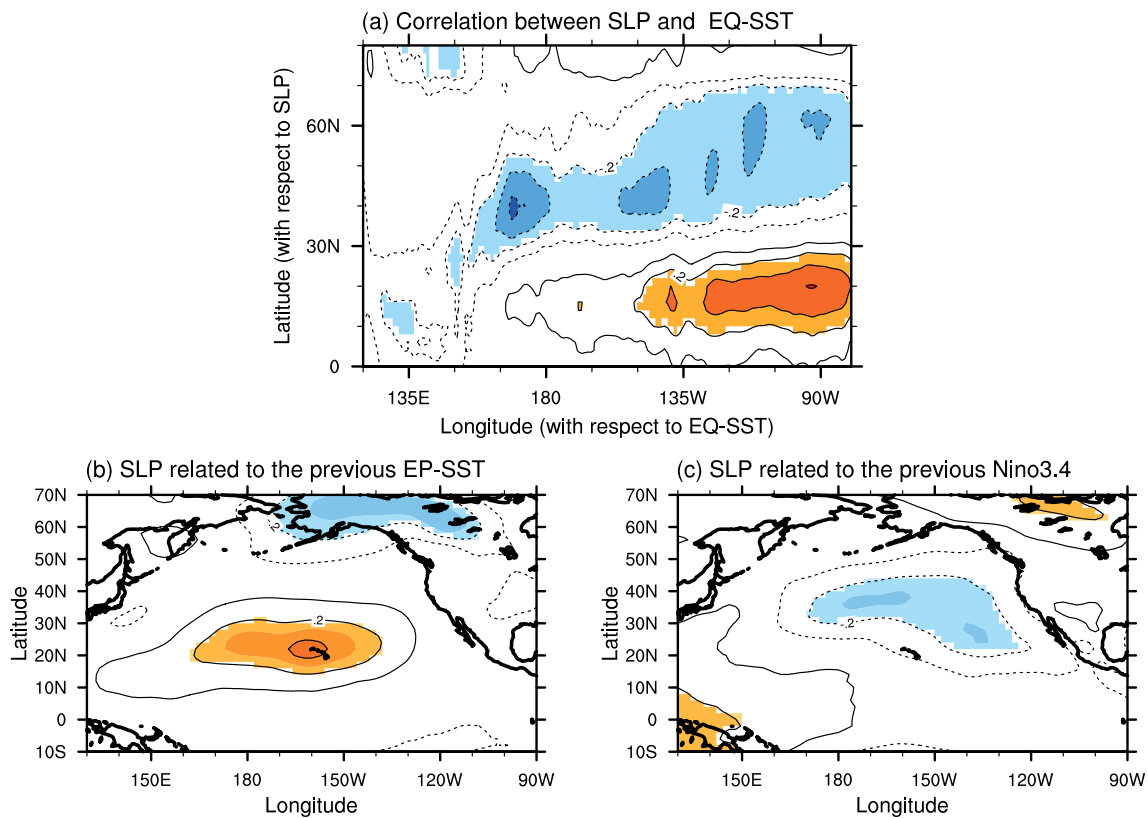


Fig. 7 **a** Cross-correlations between the April–May–June averaged SSTAs along the equatorial Pacific and the February–March–April averaged SLP anomalies over the North Pacific 1 year later; Correlation maps between the SLP anomalies and **b** the SSTAs in the eastern tropical Pacific (EP-SST) that are filtered the linear effect of

the Niño3.4 indices and **c** Niño3.4 indices that are filtered the linear effect of the EP-SST. In Figure a, the SSTAs are meridionally averaged between 5° S and 5° N, and the SLP anomalies are zonally averaged between 170° W and 160° W. Correlations above 95% confidence are shaded

equatorial Pacific in April–May–June (when the precursory signal of the EP-cooling mode usually arises) and the SLP anomalies (zonally averaged over 170° W– 160° W) over the North Pacific in February–March (when the NPO peaks) in the next year. As shown in Fig. 7a, the SSTAs in the eastern equatorial Pacific (EP-SST) are significantly correlated with the SLP over the North Pacific, presenting a negative correlation with the area north of 30° N and a positive correlation to the south. This means that the NPO is related to the previous negative EP-SST. However, since the EP-SST is directly link to the ENSO signals, one may wonder whether ENSO or EP-cooling mode can trigger the NPO event. To this end, the correlation is conducted between the SLP and the EP-SST, where the latter is removed by the liner effect of the Niño3.4 indices. The partial correlation map shows that the EP-SST still possesses high negative correlations to the NPO when the ENSO are removed (Fig. 7b). That is, the EP-cooling mode has the potential to trigger a NPO-like atmospheric mode off the tropical Pacific through teleconnection mechanism, where the NPO can induce the occurrence of the CP-El Niño (Yu and Kim 2011; Pegion and Alexander 2013; Yeh et al. 2015).

We also conduct composites of the EP-cooling mode and its following air–sea states to verify the former mentioned possible mechanisms. Results are shown in Figs. 8 and 9. Consistent with the correlation analyses, the occurrence of the EP-cooling mode excites basin-scale east wind anomalies (Figs. 8a and 9b), leading to the accumulation of ocean in the western tropical and the transportation of warm water to the subtropical Pacific (Fig. 8b, d, near 10° N). Meanwhile, the EP-cooling mode can act on the SLP in the north tropical Pacific in the spring of the next year and warm up the northeastern part of the north tropical Pacific as a VM-like footprint (Fig. 9d). Such warming signal gradually invades into the central tropical Pacific leading to a CP-El Niño event (Fig. 9f). Combined the former composite and correlation analyses, it shows that the transition from the EP-cooling mode to the CP-El Niño event is related to the basin-scale air–sea coupling in the tropical Pacific and its induced NPO in the north tropical Pacific.

In fact, not all NPOs can force the ocean to influence the central tropical Pacific (e.g., 2002 CP-El Niño event), while EP-cooling-induced NPOs do exert such influence. It is noted that the footprint over the ocean imprinted by the

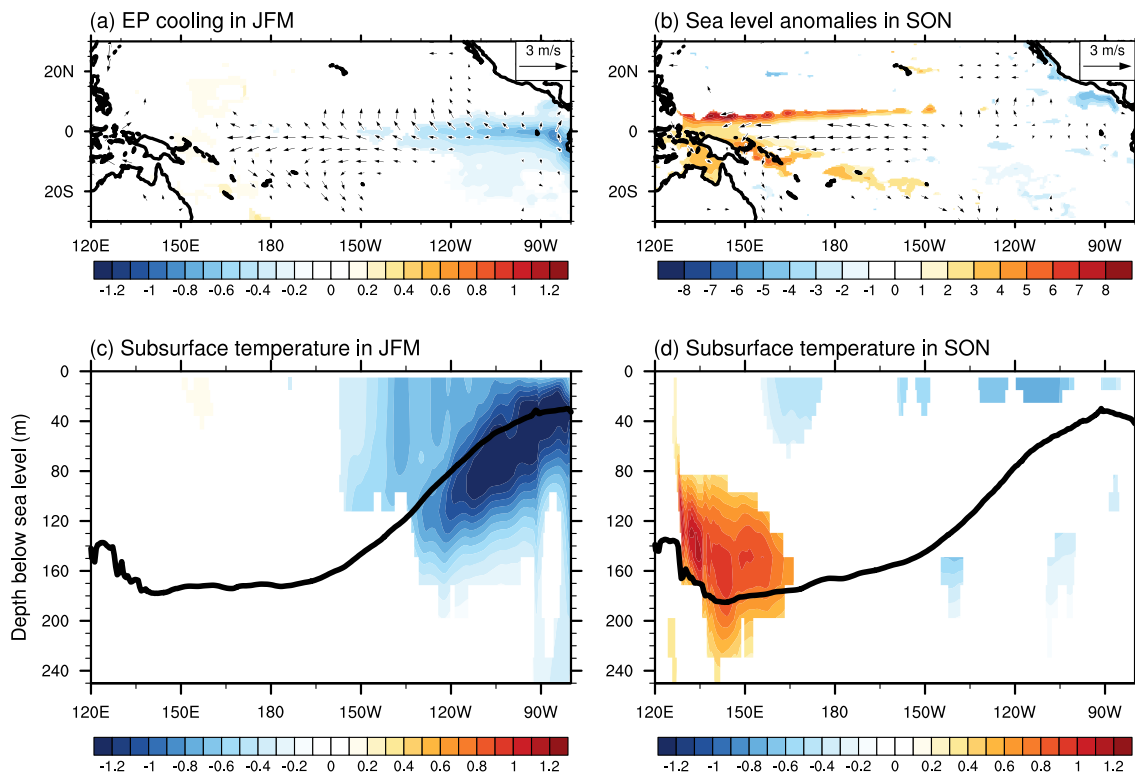


Fig. 8 Composites of **a** EP-cooling-related winter (JFM) SST and wind anomalies, **b** EP-cooling-induced SL anomalies in September–October–November, **c** EP-cooling-related subsurface temperature anomalies in winter and **d** EP-cooling-induced subsurface temperature anomalies in September–October–November. Here, the EP-cooling mode is determined as the SSTAs in the eastern tropical Pacific

(averaged over the region 110° W–80° W, 5° S–5° N) during winter and spring (i.e., January–June) less than -0.7 its standard deviation and especially less than those in the central tropical Pacific. The year of EP-cooling mode is therefore identified and a composite analysis is finally made for the climate variables as well as the following year climate states. The results that pass 90% confidence level are shown

NPO, i.e., the VM, is an important interannual variability of the SST in the North Pacific that transmits the information of the North Pacific to the tropical Pacific. To elucidate the role of the VM that is related to the EP-cooling mode, the lag correlations with the VM index (VMI; i.e., the second principle of SSTA in the north tropical Pacific) and the VMI unrelated to the EP-cooling mode (calculated by Eq. (1)) are calculated with the SST, surface wind, latent heat flux (LHF) and subsurface temperature anomalies. As shown in Fig. 10a, the VM is overlaid by basin-scale cyclone anomalies and possesses a positive SSTA in the North Pacific and a negative SSTA in the Northwest Pacific, which is consistent with the result of Ding et al. (2015b). The south band of the VM with the positive SSTA interacts with the corresponding anomalous southwesterly and tends to span southwestward, finally forcing the warming SST to invade the tropical Pacific through WES feedback, as indicated by the strong positive correlation between the VMI and LHF in the subtropical Pacific (see Fig. 10c). Then, this warming SST is further forced by the VM-related equatorial wind anomaly and gradually yields CP-El Niño (Fig. 10e). When removing the linear effect of the EP-cooling mode, the structure of

the VM changes and the CP warming event does not occur (Fig. 10b, d, f). Specifically, the correlation of the VM to the SSTA in the Northwest Pacific is weaker when the linear effect of the EP-cooling mode is filtered, indicating that the zonal gradient of the SSTA in the subtropical Pacific induced by the VM is reduced, which results in a decrease in westerly anomalies over the central North Pacific. Thus, as reflected in the comparison between Fig. 10c, d, without the previous EP-cooling mode, the strength of the WES feedback that maintains the development of the SSTA is largely weakened as the ocean obtains less heat flux. In a weak WES feedback system, the positive SSTA of the VM and relevant westerly anomalies that tend to extend into the central equatorial Pacific are delayed. In this situation, there is almost no warming signal along the equatorial Pacific in fall (Fig. 10f) and the CP-El Niño event fails to take shape.

For comparison, the composites of EP-cooling related and unrelated VM are implemented, which are shown in Fig. 11. In the composite analysis, the VM events are defined as when the VMI is larger than 0.3 times of its standard deviation during FMA. The composite VM

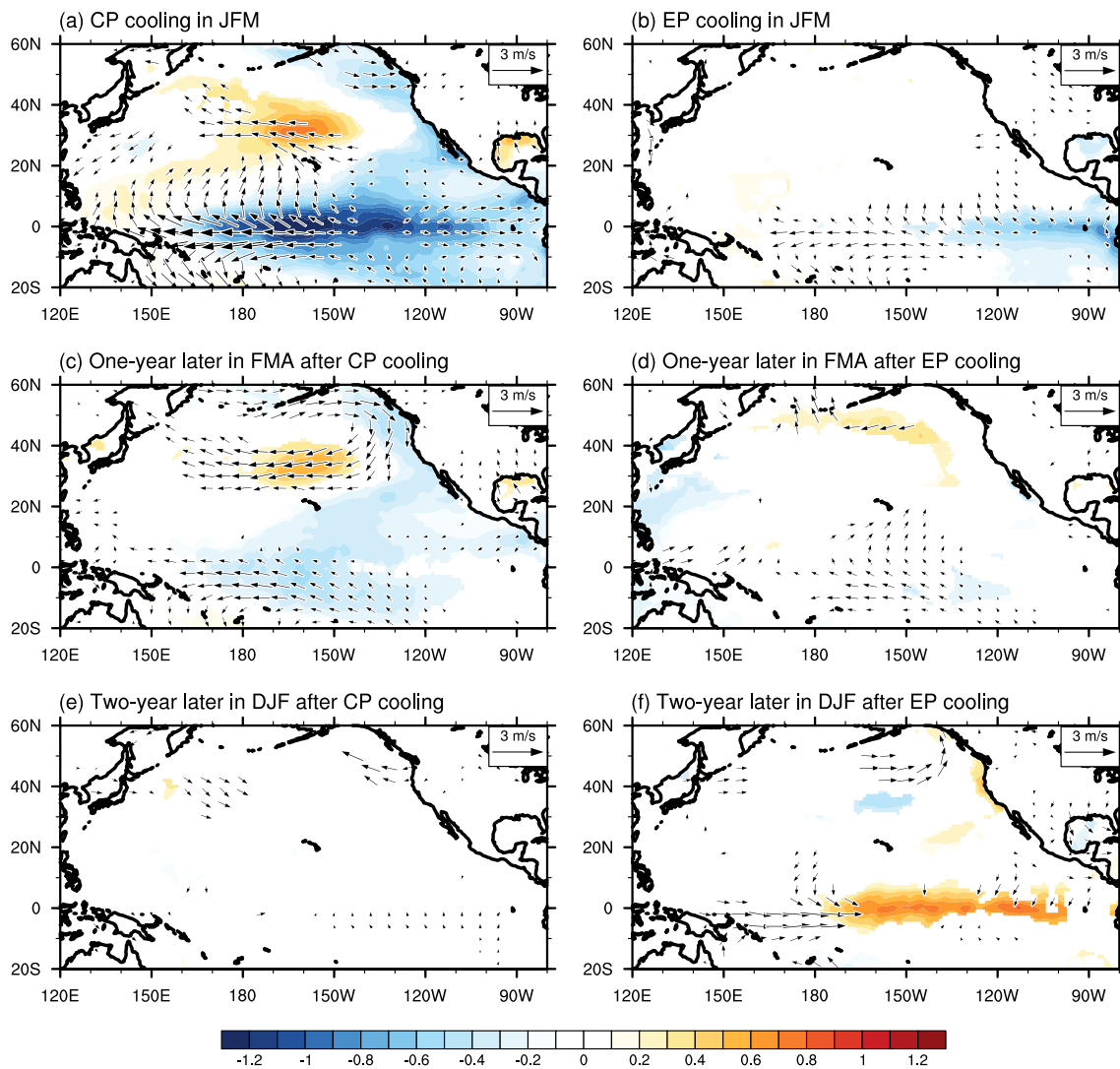


Fig. 9 Composites of the SSTA and surface wind anomalies that are induced by the CP-cooling and EP-cooling modes. The composite for CP-cooling mode is made when the SSTAs in the central tropical Pacific (averaged over the region 175°W – 110°W , 5°S – 5°N) are

less than -0.8 its standard deviation during winter and spring and simultaneously lower than the values in the eastern tropical Pacific. Only the results that pass the 90% confidence level are shown

events that are associated with the previous EP-cooling mode exhibit significant positive SSTAs and west wind anomalies in the north tropical Pacific (Fig. 11e). This kind of VM acts to warm up the central tropical Pacific at the end year of VM (Fig. 11f). In contrast, the composite VM events without the previous EP-cooling mode possess much weaker SSTA than the EP-cooling mode related VM events (Fig. 11b, e). Hence, such weak VM is not strong enough to influence the central tropical Pacific and offset the tropical cooling signal. From the above, it is known that the EP-cooling mode is an important preceding factor to enhance the linkage between the VM and CP-El Niño events.

4.2 Why a CP-cooling mode cannot lead to a CP-El Niño?

Since the EP-cooling mode can evolve into a CP-El Niño event through tropical air–sea coupling and teleconnection between the tropical and North Pacific, it naturally leads us to question why a CP-cooling-like SSTA pattern does not produce such an effect.

According to the lag-correlation analysis (Fig. 7a), the lagged negative SLP anomalies in the high latitudes tend to shift equatorward in response to the movement of the equatorial SSTA from the eastern Pacific to the western Pacific. Hence, the negative SSTA in the central tropical Pacific is unable to trigger a NPO but favors the formation

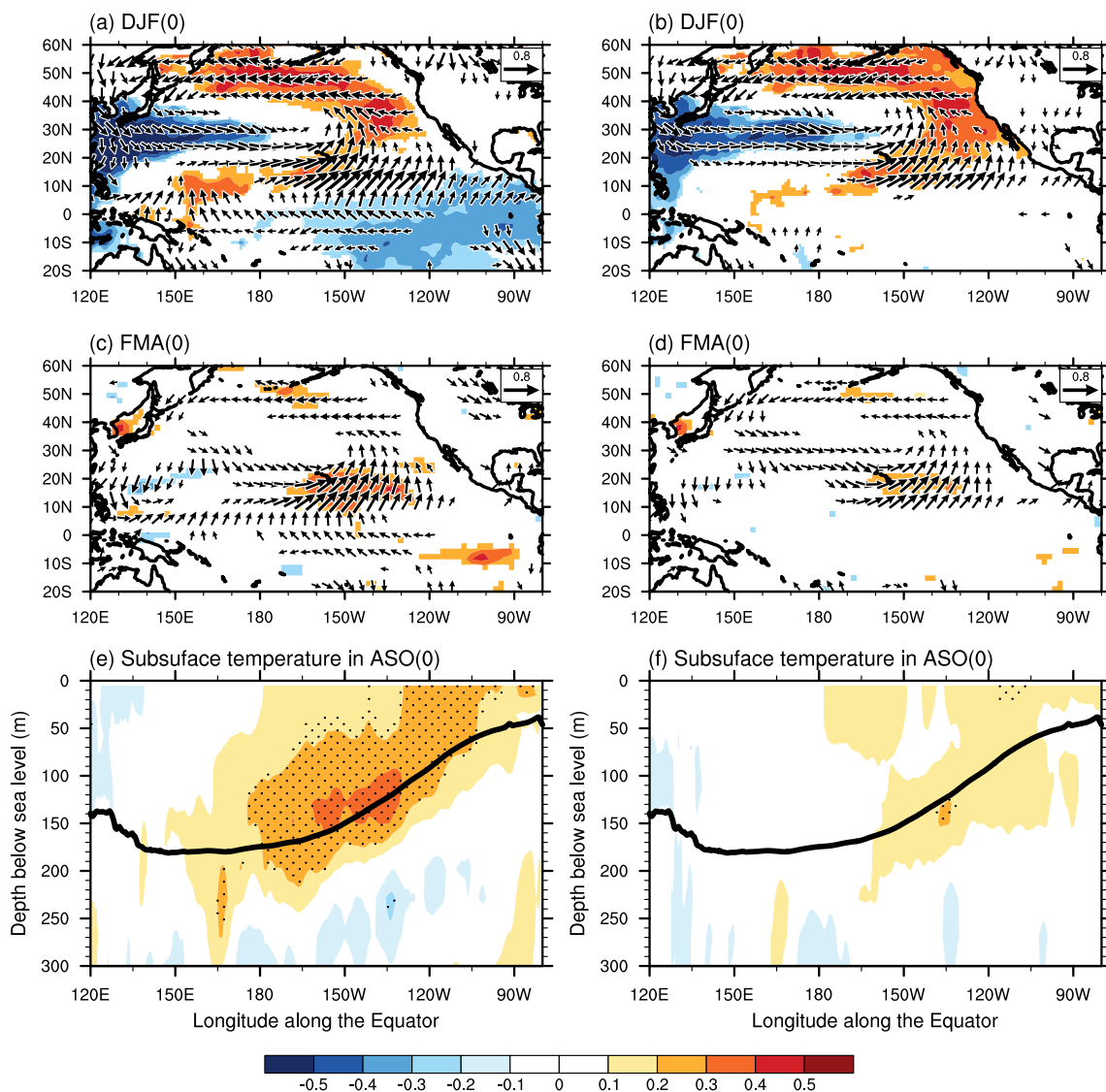


Fig. 10 Correlations of the VMI in spring (i.e., February–March–April) with the **a** surface wind (vector) and SSTA (shaded) during December–January–February, **c** surface wind and latent heat flux anomaly (shaded) during February–March–April and **e** subsurface temperature during August–September–October. The right panels

(b,d,f) show the correlation of residual VMI that filters the linear effect of the leading SSTAs in the eastern tropical Pacific. The black curves in **e** and **f** denote the depths of the thermocline along the equator. The correlations pass 95% confidence are shown in **a–d** and dotted in **e** and **f**

of a negative Aleutian low. When we filter the effect of the EP-SST on the Niño3.4, we find the residual Niño3.4 indices still present significant negative correlations to the SLP anomalies over the Aleutian region (Fig. 7c). To better describe the distinct effect of EP-cooling and CP-cooling on the North Pacific, the composites of the air–sea evolution induced by the CP-cooling and EP-cooling modes are conducted and displayed in Fig. 9. The CP-cooling triggered atmospheric variability over the North Pacific is significantly differed to that induced by the EP-cooling. For the CP-cooling mode, the central tropical Pacific cooling cooperated with the anticyclone flow over the North Pacific (i.e., negative Aleutian low mode) persists for 1 year (see

Fig. 9a, c). Without the blessing of the positive SSTAs in the eastern subtropical Pacific, the CP-El Niño event hardly occurs (see Fig. 9e).

The response of tropical wind anomalies to the CP-cooling mode is also different from that to the EP-cooling mode. The CP-cooling mode tends to promote anomalous divergence of surface wind in the central tropical Pacific (Fig. 9a). Then, the CP-cooling-induced westerly anomalies in turn lead to eastern ocean transport converging to the equator, thus triggering the upwelling Rossby wave off the eastern equatorial Pacific (not shown). This kind of cooling wave transmits westward and acts to maintain

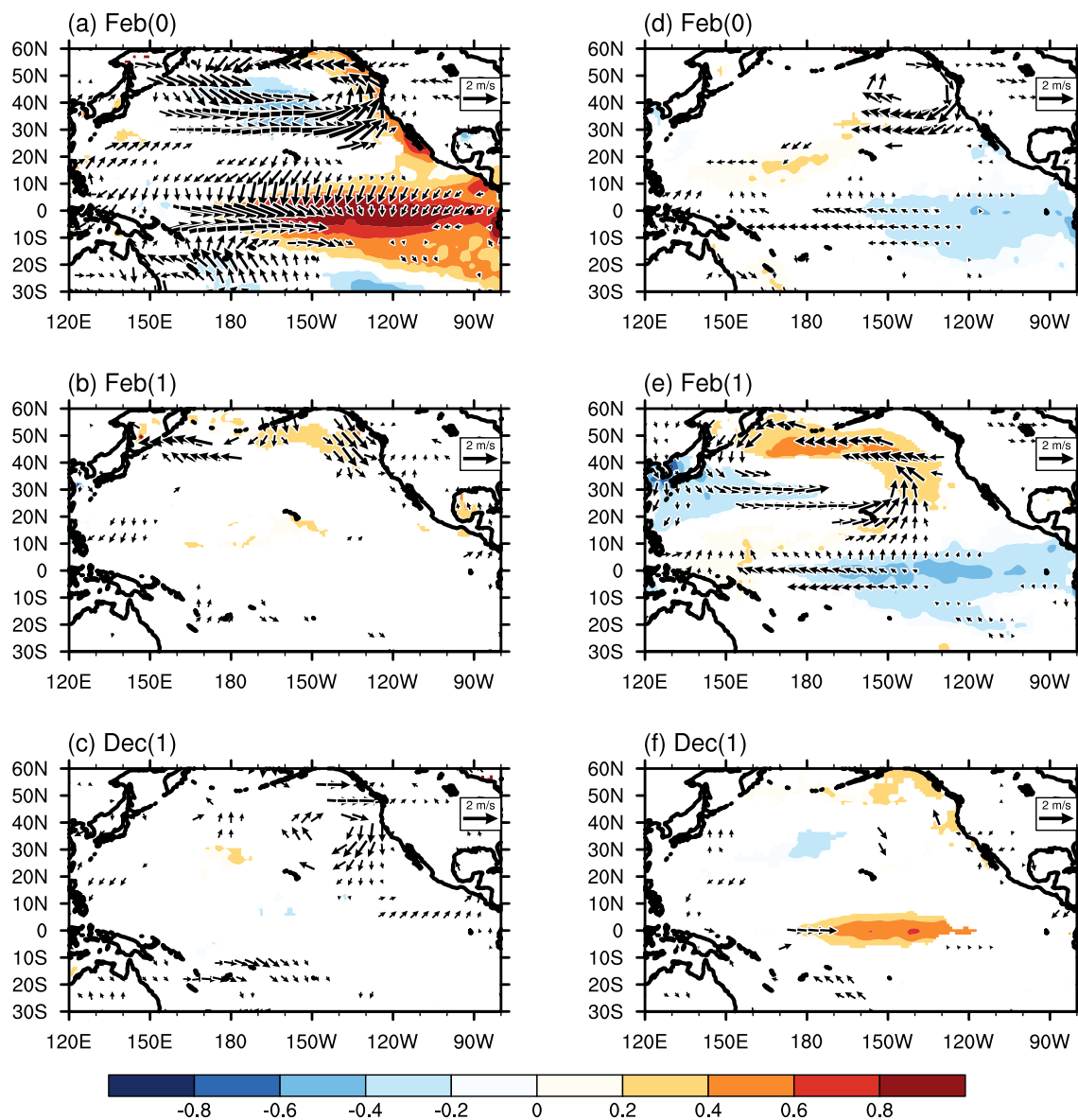


Fig. 11 Composites of SSTA and wind anomalies. The right panels are those related to the VM and EP-cooling mode, and the right panels are those related to the VM but unrelated to the EP-cooling mode. Only composites that pass 90% confidence are shown

the negative SSTA in the central Pacific. Therefore, a CP-cooling event (i.e., CP-La Niña) usually persists to the next year (Hu et al. 2014) and then disappears (Fig. 9e). Although the upwelling Rossby wave is also found in the EP-cooling case, this wave is delayed compared with the CP-cooling case as it is a kind of reflected Kelvin wave and a part of the wave energy is dissipated. Thus, the cooling wave has little effect on the subtropical Pacific but is defeated by the anomalously warm water that is induced by the anomalous easterlies. Above all, the CP-cooling mode does not favor a transition to a CP-EI Niño event while the EP-cooling mode does.

5 Hindcast experiments of ENSO with the SSTAs in the eastern tropical Pacific as a predictor

The above results have shown that the EP-cooling mode can serve as a useful precursory signal of CP-EI Niño events rather than EP-EI Niño events, which may indicate that the leading SSTAs in the eastern tropical Pacific are a useful predictor to improve the ENSO predictions as well as the CP-EI Niño predictions. To confirm this inference, a twin experiment regarding the regression-based hindcast is carried out. Previous studies (e.g., Fang and Mu 2018; Lai et al. 2018) have documented that wind and heat

content indices are useful predictors of ENSO events and constructed a linear regression air–sea coupling model as in Eq. (5) for ENSO predictions.

$$\text{Model 1 : } Nino^m = \alpha \cdot ZW^{MAM} + \beta \cdot HC^{MAM} + \varepsilon. \quad (5)$$

where $Nino^m$ is the predicted Niño index (i.e., Niño3, Niño4, or Niño3.4 index) in month m , ZW^{MAM} and HC^{MAM} represent the springtime (i.e., March–April–May) zonal wind anomaly over the western tropical Pacific (averaged over the region $150^\circ \text{ E}–160^\circ \text{ W}$, $10^\circ \text{ S}–10^\circ \text{ N}$) and equatorial thermocline fluctuation (defined as a depth of 20° C sea water temperature averaged in region $120^\circ \text{ E}–80^\circ \text{ W}$, $2^\circ \text{ S}–2^\circ \text{ N}$), respectively. The relevant coefficients α , β and ε are optimally obtained by training Model-1 from 1960–2010. Now, we include the leading SST signal of the eastern tropical Pacific in Model 1 with training from 1960–2010 and formulate Model-2 as shown in Eq. (6).

$$\text{Model 2 : } Nino^m = \alpha \cdot ZW^{MAM} + \beta \cdot HC^{MAM} + \gamma \cdot EP^{prev} + \varepsilon, \quad (6)$$

where EP^{prev} is the leading SSTA (defined as the SSTA averaged over the region $110^\circ \text{ W}–70^\circ \text{ W}$, $5^\circ \text{ S}–5^\circ \text{ N}$ during the last year). These predictor (i.e., ZW^{MAM} , HC^{MAM} , and EP^{prev}) are independent of each other, with correlations less than 0.2 at 99% confidence.

Note that the formulated Model 1 is demonstrated to possess high skills in ENSO predictions. Here, a comparison between Models 1 and 2 shows that the leading SST signal of the eastern tropical Pacific can further improve the prediction skill of the SSTA in the central tropical Pacific, as indicated by the correlation of the wintertime Niño4 index increasing from 0.65 to 0.72 (see Fig. 12b, e). For the Niño3 index, the correlation only increases from 0.76 to 0.77 (see Fig. 12a, d). In contrast, the prediction skills towards the CPI is increased by nearly 25% from 0.43 to 0.45. Evidently, the leading SST signal in the eastern tropical Pacific is useful for improving the ENSO prediction skill, especially for the CP-El Niño events.

The effect role of previous EP-SST in ENSO predictions holds in the cross-validation experiments. We firstly train the models using the data from the period 1960–1985 and predict the SSTA during 1985–2010 for validation. Then, the model that is trained using the data from 1985–2010 is used to predict the SSTA during 1960–1985. The prediction skills are indicated in Fig. 13. Clearly, the Model 2 shows better performance than the Model 1 in ENSO predictions during either the training periods or the prediction periods, especially for the CPI predictions. The cross-validation experiments shed light on the important role of the leading EP-SST in the prediction of SSTA in the central tropical Pacific as well as the prediction of CP-El Niño events.

6 Conclusions and discussion

The CP-El Niño, exerting a different global climate effect compared to the traditional type of El Niño, occurs frequently since the twelve first century. Besides the strength of El Niño, predicting its horizontal pattern is thus important. While due to the limitation of climate models, most models lose skills in predicting the El Niño type after one season (e.g., Hendon et al. 2009; Tao et al. 2020), especially for the CP-El Niño prediction. One of main reasons is the lack the knowledge of the originations of EP- and CP-El Niño and their evolution mechanisms.

To this end, the present study firstly explores the CP-El Niño precursory signal using the reanalysis data. It is found that an EP-cooling mode that presents a negative SSTA in the eastern tropical Pacific is much more likely to induce the onset of CP-El Niño events 1 year later. By observing previous condition of the El Niño events whether are the EP-cooling type or not in the tropical Pacific, the types of El Niño are well pre-identified. Then, the simulated CP-El Niño events with the NFSV-ICM are analyzed as well as the CMIP5 outputs. Those simulations pointed out that the EP-cooling mode is favored to warm up the central tropical Pacific. It is therefore confirmed that the EP-cooling mode in the tropical Pacific can be served as a reliable predictor for distinguishing the type of El Niño that will occur. Particularly, based on the hind-cast experiments with linear regression ENSO models, it is shown that adding the previous SST signal as predictor can further improve the CP-El Niño predictions.

Physically, the transition from the EP-cooling mode to a CP-El Niño is related to the basin-scale easterly wind anomalies in the tropical Pacific induced by the EP-cooling mode and the NPO-like atmospheric anomalies in the North Pacific. The occurrence of the EP-cooling mode enhances the Walker circulation so that a basin-scale easterly wind anomaly is triggered to transport warm water poleward and westward. Then, the EP-cooling mode tends to induce a PMM-like SSTA pattern that has the potential to generate the CP-El Niño event under the condition of strong zonal advection feedback in the central western tropical Pacific. Moreover, the EP-cooling mode tends to trigger the NPO-like atmospheric anomaly, which forces the Pacific ocean to warm up the central tropical Pacific by the oceanic path of the VM.

An emphasis is that when filtering the effect of the EP-cooling mode, the residual VM can hardly induce a CP-El Niño but tends to generate a weak EP-El Niño event due to the weak WES feedback. The EP-cooling mode is clearly a better precursory signal of the CP-El Niño than the VM or NPO because the latter two can also cause an EP-El Niño event (Ding et al. 2017). What is noteworthy is that

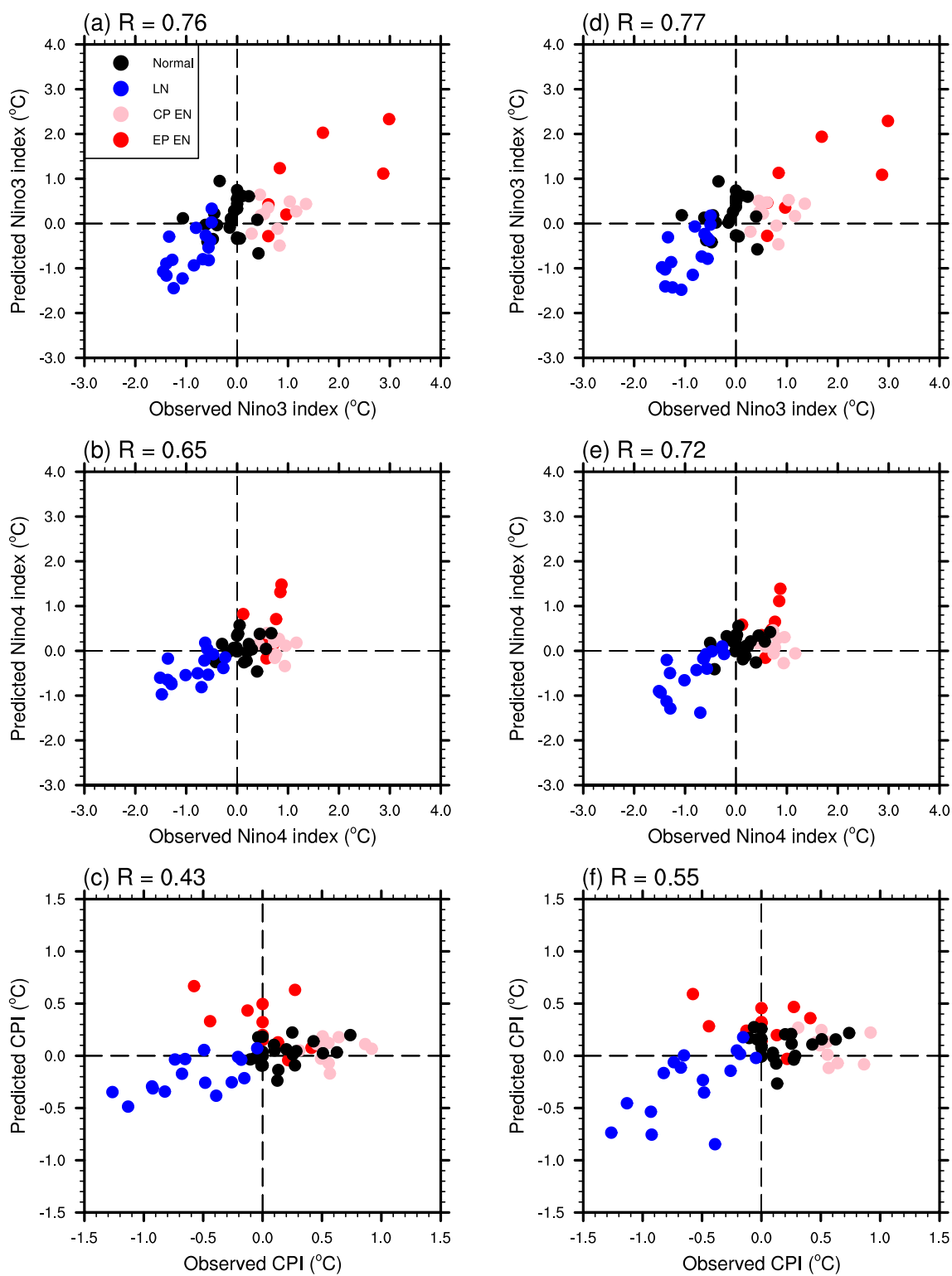


Fig. 12 Relations between the predicted and observed Niño indices in winter during 1960–2010. The CPI, i.e., the CP-El Niño index, is obtained by the method proposed by Ashok et al. (2007). The left

panels are derived from the Model 1 prediction, and the right panels are from the Model 2 prediction

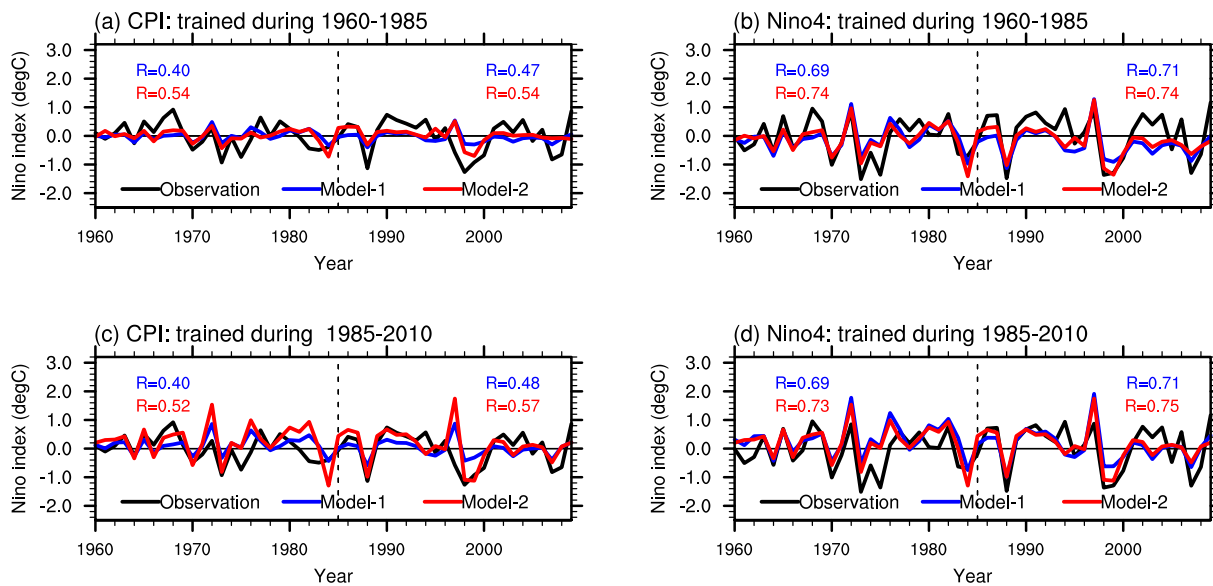
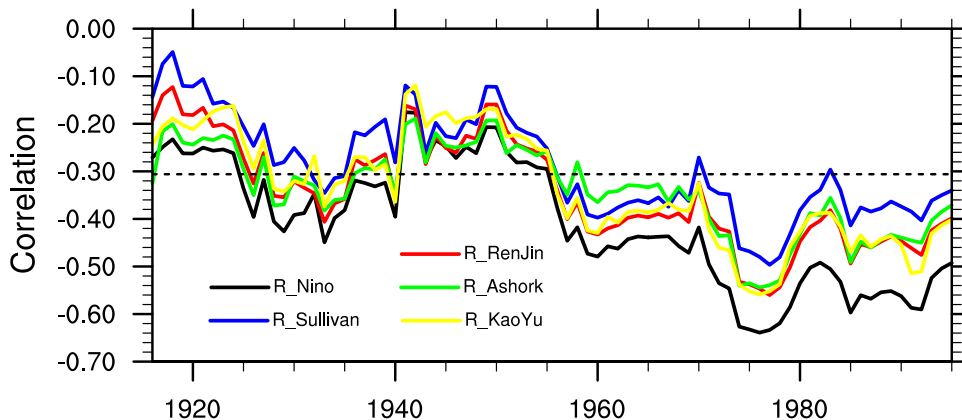


Fig. 13 Times series of Niño indices derived from observation and model predictions. **a, b** are from the predictions by the models that are trained during 1960–1985, **c, d** are from the models that are trained during 1985–2010. The correlations between predicted and

observed Niño indices during the period 1960–1985 and the period 1985–2010 are listed over the left and right part of each panel, respectively. The black curves are the observation. The red and blue curves are prediction results from Model 1 and Model 2, respectively

Fig. 14 The decadal variability of correlations between wintertime CPI and leading EP-SST under a 30-year sliding window. Each colored curve is calculated by using the CPIs that proposed by the corresponding researchers



the CP-El Niño is more and more related to the precursory EP-cooling mode in recent decades. As show in Fig. 14, the connection between the previous EP-signal and the CP-El Niño is lowest during 1900–1960. While, in recent decades, the CPI is significantly correlated to the previous EP-signal, where the correlation is up to -0.6 . Thus, a more attention is suggested to be payed to the EP-cooling mode so as to improve the El Niño diversity prediction in the situation of the global warming, especially considering the frequent occurrences of CP-El Niño.

The enhanced correlation between previous EP-SST and CP-El Niño may be as a consequence of enhanced interaction between tropical Pacific and North Pacific. According to the lag-correlation maps (Fig. 15a), the SST anomalies along the equator hardly influenced the atmospheric variability

over the North Pacific at about 1-year lead time before the 1960s. While, after 1960s, the EP-SST presents significant positive (negative) correlation to the SLP over the south (north) part of the North Pacific (Fig. 15b). From this point, the EP-cooling mode is recently easier to trigger a NPO-like SLP anomaly over the North Pacific, thus leading to a much more robust relationship between EP-cooling mode and the following CP-El Niño events. The enhanced response of the North tropical Pacific to the equatorial SST anomalies may explain why NPO has changed to the dominant variability of SLP over the North Pacific in recent decades (Yeh et al. 2015).

What favors for the EP-cooling mode is not concerned here but of interest still. According to previous studies, the frequent occurrence of CP-El Niño events is associated

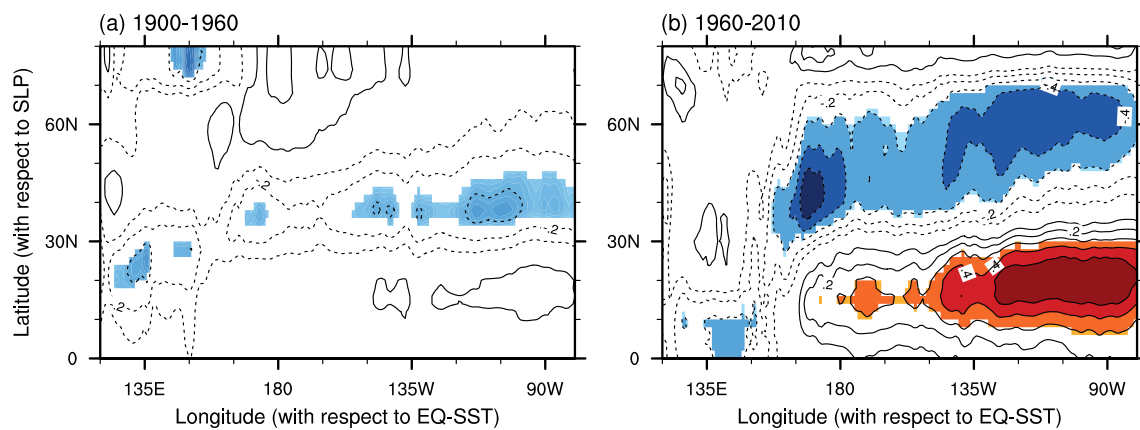


Fig. 15 Same as Fig. 7a but the lag-correlations are obtained during the period from 1900 to 1960 in **a** and from 1960–2010 in **b**

with a climatological La Niña-like background and a climatological shallower thermocline of the tropical Pacific (Choi et al. 2011) due to the strong equatorial trade wind and cross-equatorial wind over the eastern Pacific (Hu and Fedorov 2018). These climatological states may provide a favorable background for the occurrence of the EP-cooling mode. Besides, stochastic winds, such as synoptic-scale surface easterly wind surges, also play a role in the formulation of EP-cooling events (Chiodi and Harrison 2015), which may provide another possible source of EP-cooling mode. In any case, longer observation datasets and more numerical experiments are still needed to verify the precursory EP-cooling mode and to explore its origination in future studies. Despite the various horizontal type of El Niño, the diversities in the strength and duration period of El Niño are equally important to be profound studied as well as their specific precursors. These researches including the current study are expected to be helpful for having insights into the variability of short-term climate and then to promote the prediction levels.

Acknowledgements The authors appreciate the reviewers very much for their insightful comments and suggestions. This work was supported by the National Natural Science Foundation of China (Grant Nos. 41525017, 41930971, and 41690124). The authors appreciate the Climate Model Intercomparison Project (CMIP) that provides the model output freely (downloaded from <https://esgf-node.llnl.gov/search/cmip5/>).

Data availability The monthly SST data from the Met Office Hadley Centre Sea Ice and Sea Surface Temperature (HadISST) dataset were obtained at the website <http://www.metoffice.gov.uk/hadobs/hadisst/data/download.html> (Rayner et al. 2003); the subsurface ocean data are obtained from the Simple Ocean Data Assimilation (SODA, version 2.2.4) (Carton and Giese 2008; http://apdrc.soest.hawaii.edu/datadoc/soda_2.2.4.php); and the surface atmospheric and heat flux data are derived from the Twentieth Century Reanalysis (20CR) (Compo et al. 2011; downloaded from <http://iridl.ldeo.columbia.edu/SOURCES/NOAA/ESRL/PSD/rean20thcent/>). The Climate Model

Intercomparison Project (CMIP) are downloaded from <https://esgf-node.llnl.gov/search/cmip5/>).

References

- Alexander MA, Blade I, Newman M, Lanzante JR, Lau NC, Scott JD (2002) The atmospheric bridge: the influence of ENSO teleconnections on air–sea interaction over the global oceans. *J Clim* 15(16):2205–2231
- Ashok K, Behera SK, Rao SA, Weng HY, Yamagata T (2007) El Niño Modoki and its possible teleconnection. *J Geophys Res Oceans* 112:C11007
- Bjerknes J (1969) Atmospheric Teleconnections from Equatorial Pacific. *Mon Weather Rev* 97(3):163–172
- Bond NA, Overland JE, Spillane M, Stabeno P (2003) Recent shifts in the state of the North Pacific. *Geophys Res Lett.* <https://doi.org/10.1029/2003GL018597>
- Bretherton CS, Widmann M, Dymnikov VP, Wallace JM, Blade I (1999) The effective number of spatial degrees of freedom of a time-varying field. *J Clim* 12(7):1990–2009
- Capotondi A, Sardeshmukh PD (2015) Optimal precursors of different types of ENSO events. *Geophys Res Lett* 42(22):9952–9960
- Carton JA, Giese BS (2008) A reanalysis of ocean climate using Simple Ocean Data Assimilation (SODA). *Mon Weather Rev* 136(8):2999–3017
- Chiang JCH, Vimont DJ (2004) Analogous Pacific and Atlantic meridional modes of tropical atmosphere–ocean variability. *J Clim* 17(21):4143–4158
- Chiodi AM, Harrison DE (2015) Equatorial Pacific easterly wind surges and the onset of La Niña events. *J Clim* 28(2):776–792
- Choi J et al (2011) The role of mean state on changes in El Niño’s flavor. *Clim Dyn* 37(5–6):1205–1215
- Compo GP et al (2011) The Twentieth Century Reanalysis Project. *Q J R Meteorol Soc* 137(654):1–28
- Ding RQ, Li JP, Tseng YH (2015a) The impact of South Pacific extratropical forcing on ENSO and comparisons with the North Pacific. *Clim Dyn* 44(7–8):2017–2034
- Ding RQ, Li JP, Tseng YH, Sun C, Guo YP (2015b) The Victoria mode in the North Pacific linking extratropical sea level pressure variations to ENSO. *J Geophys Res Atmos* 120(1):27–45

- Ding RQ, Li JP, Tseng YH, Sun C, Zheng F (2017) Linking a sea level pressure anomaly dipole over North America to the central Pacific El Niño. *Clim Dyn* 49(4):1321–1339
- Duan WS, Zhou FF (2013) Non-linear forcing singular vector of a two-dimensional quasi-geostrophic model. *Tellus A* 65:256–256. <https://doi.org/10.3402/tellusa.v65i0.18452>
- Duan WS, Tian B, Xu H (2014) Simulations of two types of El Niño events by an optimal forcing vector approach. *Clim Dyn* 43(5–6):1677–1692
- Fang XH, Mu M (2018) Both air–sea components are crucial for El Niño forecast from boreal spring. *Sci Rep* 8(1):10501. <https://doi.org/10.1038/s41598-018-28964-z>
- Fedorov AV, Hu SN, Lengaigne M, Guilyardi E (2015) The impact of westerly wind bursts and ocean initial state on the development, and diversity of El Niño events. *Clim Dyn* 44:1381–1401
- Ham YG, Kug JS, Park JY (2013) Two distinct roles of Atlantic SSTs in ENSO variability: north Tropical Atlantic SST and Atlantic Niño. *Geophys Res Lett* 40(15):4012–4017
- Hendon HH, Lim E, Wang GM, Alves O, Hudson D (2009) Prospects for predicting two flavors of El Niño. *Geophys Res Lett*. <https://doi.org/10.1029/2009gl040100>
- Hu JY, Duan WS (2016) Relationship between optimal precursory disturbances and optimally growing initial errors associated with ENSO events: implications to target observations for ENSO prediction. *J Geophys Res Oceans* 121(5):2901–2917
- Hu SN, Fedorov AV (2018) Cross-equatorial winds control El Niño diversity and change. *Nat Clim Change* 8(9):798
- Hu ZZ, Kumar A, Xue Y, Jha B (2014) Why were some La Niñas followed by another La Niña? *Clim Dyn* 42(3–4):1029–1042
- Kao HY, Yu JY (2009) Contrasting Eastern-Pacific and Central-Pacific types of ENSO. *J Clim* 22(3):615–632
- Kug JS, Jin FF, An SI (2009) Two types of El Niño events: cold tongue El Niño and warm pool El Niño. *J Clim* 22(6):1499–1515
- Lai AWC et al (2018) ENSO forecasts near the spring predictability barrier and possible reasons for the recently reduced predictability. *J Clim* 31(2):815–838
- Mo KC (2000) Relationships between low-frequency variability in the Southern Hemisphere and sea surface temperature anomalies. *J Clim* 13(20):3599–3610
- Mu M, Yu YS, Xu H, Gong TT (2014) Similarities between optimal precursors for ENSO events and optimally growing initial errors in El Niño predictions. *Theor Appl Climatol* 115(3–4):461–469
- Pegion K, Alexander M (2013) The seasonal footprinting mechanism in CFSv2: simulation and impact on ENSO prediction. *Clim Dyn* 41(5–6):1671–1683
- Philander SGH (1983) El-Niño Southern Oscillation phenomena. *Nature* 302(5906):295–301
- Rayner NA, Parker DE, Horton EB, Folland CK, Alexander LV, Rowell DP, Kent EC, Kaplan A (2003) Global analyses of sea surface temperature, sea ice, and night marine air temperature since the late nineteenth century. *J Geophys Res Atmos* 108:D14. <https://doi.org/10.1029/2002JD002670>
- Ren HL, Jin FF (2011) Niño indices for two types of ENSO. *Geophys Res Lett* 38:L04704
- Rogers JC (1981) The north Pacific oscillation. *J Climatol* 1(1):39–57
- Sullivan A, Luo JJ, Hirst AC et al (2016) Robust contribution of decadal anomalies to the frequency of central-Pacific El Niño. *Sci Rep* 6(1):38540
- Taschetto AS, Sen Gupta A, Jourdain NC, Santoso A, Ummenhofer CC, England MH (2014) Cold tongue and warm pool ENSO events in CMIP5: mean state and future projections. *J Clim* 27:2861–2885. <https://doi.org/10.1175/Jcli-D-13-00437.1>
- Tao LJ, Duan WS (2019) Using a nonlinear forcing singular vector approach to reduce model error effects in ENSO forecasting. *Weather Forecast* 34:1321–1342. <https://doi.org/10.1175/WAF-D-19-0050.1>
- Tao LJ, Duan WS, Vannitsem S (2020) Improving the forecasts of El Niño diversity: a nonlinear forcing singular vector approach. *Clim Dyn* 55:739–754. <https://doi.org/10.1007/s00382-020-05292-5>
- Timmermann A et al (2018) El Niño–Southern Oscillation complexity. *Nature* 559(7715):535–545
- Vimont DJ, Battisti DS, Hirst AC (2001) Footprinting: a seasonal connection between the tropics and mid-latitudes. *Geophys Res Lett* 28(20):3923–3926
- Vimont DJ, Wallace JM, Battisti DS (2003a) The seasonal footprinting mechanism in the Pacific: Implications for ENSO. *J Clim* 16(16):2668–2675
- Vimont DJ, Battisti DS, Hirst AC (2003b) The seasonal footprinting mechanism in the CSIRO general circulation models. *J Clim* 16(16):2653–2667
- Wang C (2019) Three-ocean interactions and climate variability: a review and perspective. *Clim Dyn* 53:5119–5136
- Wang X, Tan W, Wang C (2018) A new index for identifying different types of El Niño Modoki events. *Clim Dyn* 50:2753–2765. <https://doi.org/10.1007/s00382-017-3769-8>
- Wang X, Chen MY, Wang CZ et al (2019a) Evaluation of performance of CMIP5 models in simulating the North Pacific Oscillation and El Niño Modoki. *Clim Dyn* 52(3–4):1383–1394
- Wang X, Guan C, Huang RX, Tan W, Wang L (2019b) The roles of tropical and subtropical wind stress anomalies in the El Niño Modoki onset. *Clim Dyn* 52:6585–6597
- Wang B, Luo X, Yang YM, Sun WY, Cane MA, Cai WJ, Yeh SW, Liu J (2019c) Historical change of El Niño properties sheds light on future changes of extreme El Niño. *PNAS* 116(45):22512–22517. <https://doi.org/10.1073/pnas.1911130116>
- Xie SP, Philander SGH (1994) A coupled ocean-atmosphere model of relevance to the ITCZ in the eastern Pacific. *Tellus A* 46(4):340–350. <https://doi.org/10.3402/tellusa.v46i4.15484>
- Yang YM, Park JH, An SI et al (2021) Mean sea surface temperature changes influence ENSO related precipitation changes in the mid-latitudes. *Nat Commun* 12:1495. <https://doi.org/10.1038/s41467-021-21787-z>
- Yeh SW, Wang X, Wang CZ, Dewitte B (2015) On the relationship between the North Pacific climate variability and the Central Pacific El Niño. *J Clim* 28(2):663–677
- You YJ, Furtado JC (2017) The role of South Pacific atmospheric variability in the development of different types of ENSO. *Geophys Res Lett* 44(14):7438–7446
- Yu JY, Fang SW (2018) The Distinct contributions of the seasonal footprinting and charged-discharged mechanisms to ENSO complexity. *Geophys Res Lett* 45:6611–6618
- Yu JY, Kim ST (2010) Three evolution patterns of Central-Pacific El Niño. *Geophys Res Lett*. <https://doi.org/10.1029/2010GL042810>
- Yu JY, Kim ST (2011) Relationships between extratropical sea level pressure variations and the Central Pacific and Eastern Pacific types of ENSO. *J Clim* 24(3):708–720
- Zebiak SE, Cane MA (1987) A model El-Niño Southern Oscillation. *Mon Weather Rev* 115(10):2262–2278
- Zhang RH, Zebiak SE, Kleeman R, Keenlyside N (2003) A new intermediate coupled model for El Niño simulation and prediction. *Geophys Res Lett*. <https://doi.org/10.1029/2003GL018010>